Environmental Pollution 251 (2019) 185–192

Contents lists available at ScienceDirect

Environmental Pollution

journal homepage: www.elsevier.com/locate/envpol

# Surface nitrous oxide concentrations and fluxes from water bodies of the agricultural watershed in Eastern China☆

Qitao Xiao [a, b], Zhenghua Hu [a, *], Congsheng Fu [b], Hang Bian [a], Xuhui Lee [c, d], Shutao Chen [a], Dongyao Shang [a]

[a] Collaborative Innovation Center on Forecast and Evaluation of Meteorological Disasters, Jiangsu Key Laboratory of Agricultural Meteorology, Nanjing University of Information Science & Technology, Nanjing, 210044, China
[b] Key Laboratory of Watershed Geographic Sciences, Nanjing Institute of Geography and Limnology, Chinese Academy of Sciences, Nanjing, 210008, China
[c] Yale-NUIST Center on Atmospheric Environment, Nanjing University of Information Science & Technology, Nanjing, 210044, China
[d] School of Forestry and Environmental Studies, Yale University, New Haven, CT, 06511, USA

ARTICLE INFO

*Article history:*
Received 26 November 2018
Received in revised form
11 April 2019
Accepted 15 April 2019
Available online 22 April 2019

*Keywords:*
Indirect emission
$N_2O$ concentrations
Emission rates
Emission factor
IPCC

ABSTRACT

Agriculture is one of major emission sources of nitrous oxide ($N_2O$), an important greenhouse gas dominating stratospheric ozone destruction. However, indirect $N_2O$ emissions from agriculture watershed water surfaces are poorly understood. Here, surface-dissolved $N_2O$ concentration in water bodies of the agricultural watershed in Eastern China, one of the most intensive agricultural regions, was measured over a two-year period. Results showed that the dissolved $N_2O$ concentrations varied in samples taken from different water types, and the annual mean $N_2O$ concentrations for rivers, ponds, reservoir, and ditches were $30 \pm 18$, $19 \pm 7$, $16 \pm 5$ and $58 \pm 69$ nmol $L^{-1}$, respectively. The $N_2O$ concentrations can be best predicted by the $NO_3^-$-N concentrations in rivers and by the $NH_4^+$-N concentrations in ponds. Heavy precipitation induced hot moments of riverine $N_2O$ emissions were observed during farming season. Upstream waters are hot spots, in which the $N_2O$ production rates were two times greater than in non-hotspot locations. The modeled watershed indirect $N_2O$ emission rates were comparable to direct emission from fertilized soil. A rough estimate suggests that indirect $N_2O$ emissions yield approximately 4% of the total $N_2O$ emissions yield from N-fertilizer at the watershed scale. Separate emission factors (EF) established for rivers, ponds, and reservoir were 0.0013, 0.0020, and 0.0012, respectively, indicating that the IPCC (Inter-governmental Panel on Climate Change) default value of 0.0025 may overestimate the indirect $N_2O$ emission from surface water in eastern China. EF was inversely correlated with N loading, highlighting the potential constraints in the IPCC methodology for water with a high anthropogenic N input.



## 1. Introduction

Nitrous oxide ($N_2O$) is a powerful and long-lived greenhouse gas and also a dominant component in the destruction of the stratospheric ozone (Ravishankara et al., 2009). The atmospheric $N_2O$ concentration is estimated to have increased by 22% since 1750, with a current concentration of 329 ppb (Davidson, 2009; Cooper et al., 2017). The increasing atmospheric $N_2O$ concentration has received considerable attention. The estimated annual global $N_2O$ emission is 13.3–18.8 Tg N $yr^{-1}$, to which agriculture contributes nearly 30% (Xu et al., 2008; Cooper et al., 2017). Importantly, agriculture is considered by far the largest source (~80%) of anthropogenic $N_2O$ via both direct emission and indirect emission (Kroeze et al., 1999; Davidson, 2009; Cooper et al., 2017).

Anthropogenic $N_2O$ input into the atmosphere from fertilized soils are defined as direct emission, while indirect emission represents $N_2O$ production in ditches, streams, and rivers induced by leaching and runoff of reactive N from agricultural areas (Mosier et al., 1998; Fu et al., 2018). Direct $N_2O$ emissions have been well documented through a large amount of field measurements (Xu et al., 2008; Shcherbak et al., 2014), while indirect emissions from

☆ This paper has been recommended for acceptance by Dr. Jörg Rinklebe.

* Corresponding author. Collaborative Innovation Center on Forecast and Evaluation of Meteorological Disasters, Jiangsu Key Laboratory of Agricultural Meteorology, Nanjing University of Information Science and Technology, 219 Ningliu Road, Nanjing, Jiangsu Province, China.
*E-mail address:* zhhu@nuist.edu.cn (Z. Hu).

https://doi.org/10.1016/j.envpol.2019.04.076
0269-7491/

agricultural watershed are less well constrained due to the scarcity of studies on this topic (Reay et al., 2003; Outram and Hiscock; Fu et al., 2018). Importantly, indirect emission is estimated to account for over one-quarter of global total agricultural $N_2O$ emissions (Reay et al. 2012; Venkiteswaran et al., 2014) and dominates the inter-annual variability of total emission (Griffis et al. 2017). Meanwhile, riverine $N_2O$ emissions, especially in agricultural areas, remain a major source of uncertainty in the global $N_2O$ budget due to the large spatiotemporal variability (Beaulieu et al. 2011; Borges et al. 2015; Audet et al., 2017). More field measurements of indirect $N_2O$ emission are needed to reduce the uncertainty and improve the reliability of the global anthropogenic $N_2O$ budget (Reay et al. 2012; Saikawa et al. 2014).

IPCC provided emission factors (EF) to estimate indirect $N_2O$ emissions resulting from fertilizer-N and manure-N loss via leaching and runoff (De Klein et al. 2006), in which global and regional $N_2O$ emissions from a water body can be calculated by multiplying the nitrogen fertilizer input or relevant anthropogenic N loading with the default EF (Hu et al., 2016; Hama-Aziz et al., 2017; Fu et al., 2018). Since 2006, the IPCC default EF values for rivers, groundwater, and estuaries were both set to 0.0025 (De Klein et al., 2006). However, studies have shown that the default EF is poorly constrained due to high variability in environmental conditions (Turner et al., 2015; Cooper et al., 2017; Griffis et al. 2017). For example, a field measurement showed that the IPCC default EF is underestimated up to nine-fold in rivers in the U.S. Corn Belt, an intensively agricultural region (Turner et al., 2015; Fu et al., 2017; Fu et al., 2018), but it is unexpectedly overestimated in an intensively agriculture area in other regions (Clough et al., 2007; Outram and Hiscock, 2012; Hama-Aziz et al., 2017). Using the default IPCC emission factor for predicting indirect $N_2O$ emissions from all rivers may be inappropriate, and more measurements are needed to accurately calculate the $EF_{5r}$ (Outram and Hiscock, 2012; Hama-Aziz et al., 2017; Tian et al., 2017).

Heavy farmland N fertilizer application in Eastern China, one of most intensively agricultural regions in the world, has led to a high N loading input in the watershed. The fertilizer N application rate is up to 600 kg N $ha^{-1}$ $yr^{-1}$ in Eastern China (Ju et al. 2009; Xing and Zhu, 2002). For comparison, the value is only approximately 100 kg N $ha^{-1}$ $yr^{-1}$ in intensively agricultural regions in the US (Griffis et al. 2017; Turner et al., 2015). Further, a large amount of farmland N-fertilizer (~280 kg N $ha^{-1}$ $yr^{-1}$) enters the watershed via runoff and leaching in Eastern China (Xing and Zhu, 2002; Yan et al. 2011), which may significantly increase the $N_2O$ production rates (Beaulieu et al. 2011). Previous studies suggested that the surface water $N_2O$ emissions in Eastern China may be very high due to the vast farmland N-fertilizer (Seitzinger and Kroeze, 1998). However, until now, limited information is available regarding the characteristics of watershed $N_2O$ dynamics in this area.

In this study, we measured the dissolved $N_2O$ concentration in water bodies in a typical agricultural watershed in Eastern China. Our objectives were to quantify the importance of agricultural watershed fueled by farmland N-fertilizer as sources of indirect $N_2O$ emission in this area, to explore the indirect $N_2O$ emission factor, and to further investigate the spatiotemporal characteristics of $N_2O$ dynamics.

## 2. Materials and methods

### 2.1. Study area

This field measurement was carried out in a typical agriculture watershed located in Eastern China (31°58′ to 32°01′N, 119°12′ to 119°14′E; Fig. S1). The watershed has previously been reported in detail (Yan et al. 2011). Briefly, there is a reservoir, three rivers, and thousands of small pond in the watershed. The average annual precipitation is 1100 mm and the mean annual temperature is 15 °C. The major annual cropping rotations are rice-wheat for the paddy fields and maize-rapeseed, respectively. There is no industry in the studied area, and agriculture is the dominant local source of anthropogenic N.

### 2.2. Sample collection and analysis

A watershed-scale sampling round was conducted in each month from October 2015 to September 2017, during which samples were taken from the surface water of the reservoir, rivers, ponds, and ditches (Fig. S1). As a whole, water samples were collected from 30 sampling sites, of which 1 site was in a reservoir, 19 sites were in rivers, 3 sites were in ponds, and 7 sites were in ditches. There are three rivers in the watershed: River 1, River 2, and River 3, respectively. Given the river length, the sampling sites were divided into two sections in River 1 (midstream and downstream) and three sections (upstream, midstream, and downstream) in River 2, respectively. It should be noted that the ditches sometimes dry up without covering water, leading to discontinuous sampling.

Each watershed-scale survey was completed over two consecutive days. The procedures of sampling and analysis have previously been reported in detail in Xiao et al., (2019). Briefly, triplicate bubble-free water samples were collected at a 20-cm depth below the surface using 300 mL glass bottles, and these bottles were transported to lab for dissolved $N_2O$ concentration analysis using the headspace equilibration method. Water samples were also collected using an organic glass hydrophore to the ammonium-nitrogen ($NH_4^+$-N), nitrate-nitrogen ($NO_3^-$-N), and nitrite-nitrogen ($NO_2^-$-N) analysis by a continuous flow analyzer (Skalar san$^{++}$, Netherlands). The water temperature, pH, specific conductance (Spc), and dissolved oxygen concentration (DO) were measured *in situ* with a multiparameter probe (YSI 650MDS, YSI Inc. Yellow Springs, OH, USA) at a 20-cm depth to be consistent with water sampling.

### 2.3. $N_2O$ fluxes and emission factor calculations

The $N_2O$ fluxes ($F_n$, μmol $m^{-2}$ $d^{-1}$, positive indications of $N_2O$ emission from water to atmosphere) was calculated using water-air gas exchange model:

$$F_n = k \times (C_w\text{-}C_{eq}) \quad (1)$$

where $C_w$ is the surface dissolved $N_2O$ concentration (μmol $m^{-3}$) in water measured by headspace equilibration method, $C_{eq}$ is the $N_2O$ concentration in water that is in equilibrium with the atmosphere at the *in-situ* temperature, and $k$ is the gas transfer coefficient. For the rivers, $k$ was calculated considering both wind and water turbulence (Clough et al., 2007):

$$k = 2.78E^{-6}au_{10}^2\left(\frac{S_c}{660}\right)^{0.5} + \sqrt{\frac{DU}{h}} \quad (2)$$

where $2.78E^{-6}$ is a conversion factor (cm $h^{-1}$ to m $s^{-1}$), $a$ is a constant (0.31), $u_{10}$ is the wind speed at a height of 10 m above the water surface, and $S_c$ is the Schmidt number for $N_2O$, $U$ is the river water velocity (m $s^{-1}$), $h$ is the average river depth (m), and $D$ is the $N_2O$ diffusion coefficient in the water. The hourly measurement of wind speed was obtained from a weather station in the watershed to calculate the $k$. The river water velocity is steady and only varies depending upon precipitation (Yan et al. 2011; Xia et al., 2013b).

For the lentic ecosystem (reservoir and ponds), the $N_2O$ transfer

velocity is mainly driven by wind speed because no surface water flow occurs. $k$ (cm $h^{-1}$) was calculated from a wind-dependent formula derived from a small shallow lake as follows (Cole and Caraco, 1998):

$$k = (S_c/660)^{-n}\,(2.07 + 0.215 \times u_{10}^{1.7}) \quad (3)$$

There is no separate equation for $k$ calculation for ditches, and Equation (3) was also used for calculating the gas transfer coefficient $k$ for ditches.

The indirect $N_2O$ emission factor (EF) for rivers, ponds, ditches, and the reservoir were calculated using the common IPCC methodology as follows (De Klein et al. 2006):

$$EF = N_2O - N\,NO_3^- - N \quad (4)$$

Where $N_2O$-N and $NO_3^-$-N are concentrations measured in rivers, ponds, ditches, and the reservoir. Equation (4) has been widely used to calculate the indirect $N_2O$ emission factor (Turner et al., 2015; Hama-Aziz et al., 2017; Tian et al., 2017).

### 2.4. Data analysis

Statistical analyses were conducted with SPSS version 18.0 (SPSS, Inc., USA).

In the study area, spring is from March to the end of May, summer is from June to August, autumn is from September to November, and winter is from December to February in next year. Simple linear and multi-linear stepwise regression analyses were performed to determine the relationships among $N_2O$, the emission factor, and independent variables (e.g., $NH_4^+$-N, $NO_3^-$-N, and $NO_2^-$-N). The entire two-year dataset was divided according to water type (e.g., rivers, ponds, ditches, and reservoir), and the difference of their mean $N_2O$ concentrations and fluxes was examined using a one-way analysis of variance (ANOVA). After completing the ANOVA test, a least significant difference (LSD) post hoc test was conducted. Differences at $p < 0.05$ were labeled as statistically significant in all analyses.

## 3. Results

### 3.1. Physical and chemical characteristics

There was no obvious variation in water temperature across different water body types in the agricultural watershed (Fig. 2S(a)). The annual mean water temperature is 19.3 °C over the two-year study period. There was a clear seasonality for water temperature, with the highest water temperature appearing in the summer (33.3 °C) and the lowest (6.3 °C) in winter. The annual mean wind speed was 2.5 m $s^{-1}$ based on the measurement from the local weather station.

In contrast to water temperature, the surface water chemical properties varied among rivers, ponds, reservoir, and ditches (Table 1 and Fig. 2S). Generally, the $NO_3^-$-N concentrations was highest in ditches with annual mean value of 1.85 mg $L^{-1}$, followed by rivers (0.99 mg $L^{-1}$), reservoir (0.54 mg $L^{-1}$) and ponds (0.47 mg $L^{-1}$). In contrast, the highest $NH_4^+$-N concentration appeared in ponds with annual mean value of 0.32 mg $L^{-1}$, followed by rivers and reservoirs. The $NO_2^-$-N concentrations in these surface water areas showed minor differences. The average DO concentration was over-saturated only in the reservoir with a value of 10.45 mg $L^{-1}$ or 110% saturation, and the annual mean values for rivers, ponds, and ditches were 6.65, 5.78, and 7.90 mg $L^{-1}$, respectively.

The $NO_3^-$-N was the dominant form of the total dissolved inorganic nitrogen (DIN) in the surface water of the agricultural watershed (Table 1). For example, the $NO_3^-$-N concentration accounted for 76%, 57%, 72%, and 92% of the total DIN concentration for rivers, ponds, the reservoir, and ditches, respectively. In addition, the surface water $NO_3^-$-N concentrations for the rivers, ponds, and reservoir showed clear seasonality with peak concentrations being observed in summer and winter (Fig. 2S(b)), coincides with the crop-planting period. There were no obvious temporal variations for $NH_4^+$-N concentration except in ponds.

### 3.2. Spatial and temporal characteristics of surface water $N_2O$ concentration

The dissolved $N_2O$ concentration in surface water varied across water body types (Fig. S3). Dissolved $N_2O$ concentrations in the ditches spanned a broad range, from 10 to 243 nmol $L^{-1}$, but varied within relatively narrow ranges of 4–172 nmol $L^{-1}$, 5–50 nmol $L^{-1}$, and 9–30 nmol $L^{-1}$ in rivers, pond, and reservoir, respectively. Meanwhile, the annual mean surface $N_2O$ concentration in ditches with a value of 63 nmol $L^{-1}$ was significantly ($p < 0.01$) higher than those in rivers (29 nmol $L^{-1}$), ponds (20 nmol $L^{-1}$), and reservoir (15 nmol $L^{-1}$). The differences of $N_2O$ concentrations between

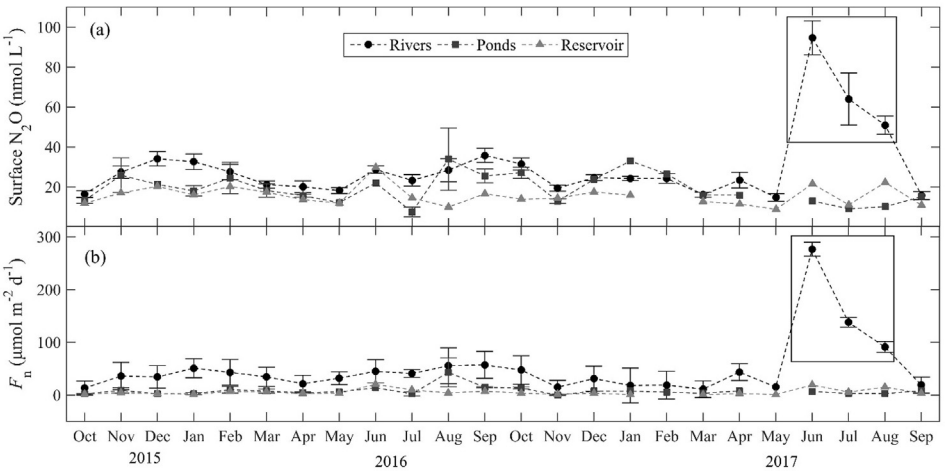


**Fig. 1.** Mean surface $N_2O$ concentration and calculated $N_2O$ flux for rivers, ponds, and reservoir during the two-year period. Error bars represent standard error. The symbols in the boxes indicate the hot moments for $N_2O$, in which samples were collected from rivers after heavy precipitation during the farming season.

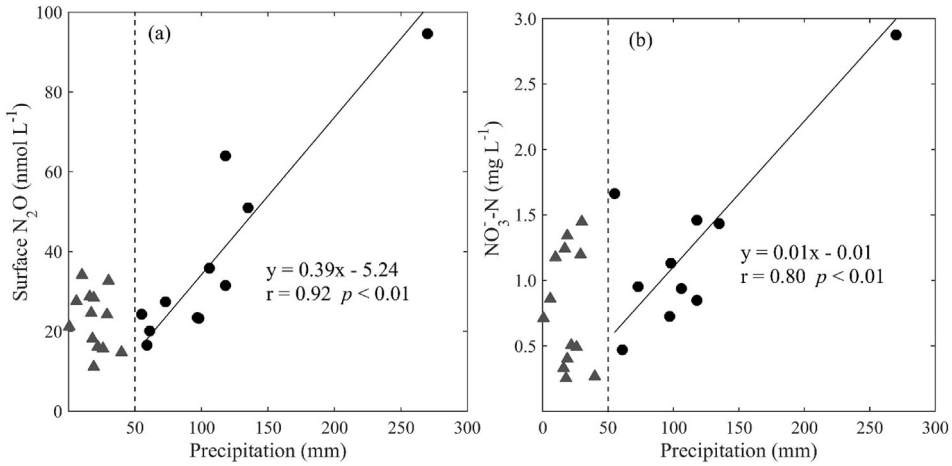


**Fig. 2.** Temporal correlation between precipitation and mean concentrations of $N_2O$ and $NO_3^-$-N in rivers. Note that the precipitation was the 10-day accumulated precipitation for each rainfall event before sampling. We assumed that major N losses from croplands induced by heavy rainfall might be transported to the rivers within 10 days based on a previous study (Yan *et al.*, 2011).

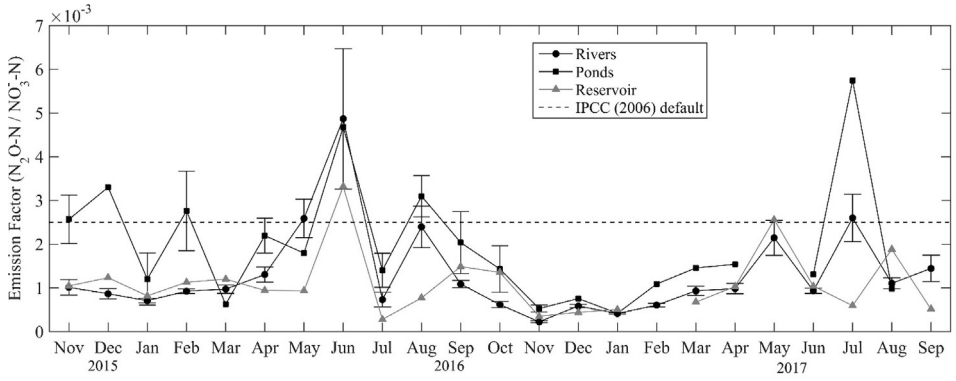


**Fig. 3.** Temporal variability in the mean emission factor ($N_2O$-N/$NO_3^-$-N ratio) for rivers, ponds, and reservoir samples collected from November 2015 to September 2017.

**Table 1**
Summary of the dissolved inorganic concentration ($NO_3^-$-N and $NH_4^+$-N), $N_2O$ concentration and fluxes, and $N_2O$ emission factor (EF) in all collected samples. The presented values are the mean ± standard deviation.

| Sample type | Season | $NH_4^+$-N (mg $L^{-1}$) | $NO_3^-$-N (mg $L^{-1}$) | $N_2O$ concentration (nmol $L^{-1}$) | $N_2O$ flux (μmol $m^{-2}$ $d^{-1}$) | EF |
|---|---|---|---|---|---|---|
| Rivers | overall | 0.26 ± 0.15 | 0.99 ± 0.59 | 30 ± 18 | 49.6 ± 55.8 | 0.0013 ± 0.0010 |
| | spring | 0.16 ± 0.05 | 0.49 ± 0.21 | 19 ± 3 | 26.3 ± 12.4 | 0.0015 ± 0.0007 |
| | summer | 0.34 ± 0.15 | 1.17 ± 0.94 | 48 ± 28 | 107.9 ± 90.4 | 0.0021 ± 0.0016 |
| | autumn | 0.24 ± 0.13 | 1.03 ± 0.38 | 24 ± 8 | 31.3 ± 18.4 | 0.0009 ± 0.0005 |
| | winter | 0.30 ± 0.21 | 1.26 ± 0.27 | 28 ± 4 | 32.8 ± 13.0 | 0.0007 ± 0.0002 |
| Ponds | overall | 0.32 ± 0.40 | 0.47 ± 0.46 | 19 ± 7 | 8.0 ± 8.6 | 0.0020 ± 0.0014 |
| | spring | 0.34 ± 0.43 | 0.39 ± 0.33 | 16 ± 3 | 5.8 ± 2.0 | 0.0015 ± 0.0006 |
| | summer | 0.37 ± 0.54 | 0.20 ± 0.10 | 16 ± 10 | 11.9 ± 15.9 | 0.0029 ± 0.0020 |
| | autumn | 0.25 ± 0.24 | 0.50 ± 0.19 | 20 ± 7 | 7.9 ± 5.9 | 0.0016 ± 0.0009 |
| | winter | 0.31 ± 0.39 | 0.79 ± 0.73 | 25 ± 5 | 6.0 ± 3.1 | 0.0016 ± 0.0011 |
| Reservoir | overall | 0.19 ± 0.09 | 0.54 ± 0.33 | 16 ± 5 | 5.6 ± 5.5 | 0.0011 ± 0.0007 |
| | spring | 0.17 ± 0.04 | 0.35 ± 0.15 | 13 ± 3 | 2.8 ± 2.0 | 0.0012 ± 0.0007 |
| | summer | 0.24 ± 0.07 | 0.58 ± 0.44 | 18 ± 8 | 12.3 ± 6.9 | 0.0013 ± 0.0011 |
| | autumn | 0.18 ± 0.14 | 0.56 ± 0.34 | 14 ± 2 | 3.7 ± 2.1 | 0.0010 ± 0.0005 |
| | winter | 0.14 ± 0.07 | 0.70 ± 0.29 | 18 ± 2 | 3.0 ± 2.4 | 0.0008 ± 0.0004 |
| Ditches | overall | 0.12 ± 0.15 | 1.85 ± 1.81 | 58 ± 69 | 45.2 ± 95.1 | 0.0014 ± 0.0013 |

rivers, ponds, and reservoir were insignificant ($p > 0.05$).

The $N_2O$ concentrations also varied within rivers. River 3 with the shortest transport length (Fig. S1) had the highest $N_2O$ concentration compared to River 1 and River 2. The overall mean $N_2O$ concentrations were 26, 30, and 35 for rivers 1, 2, and 3, respectively. Further analysis showed large spatial variations for the riverine $N_2O$ concentration along the current direction of the water (Fig. S4). A $N_2O$ concentration gradient from the upstream to the estuary is clearly evident. Peak $N_2O$ concentrations were typically found in the upstream of the river. The annual mean $N_2O$ concentrations in upstream, midstream, and downstream of River 2 were 45, 25, and 21 nmol $L^{-1}$, respectively. River 3 is too short to be

sampled at different locations, and samples were only taken from midstream and downstream in River 1, but the measured data also showed that the $N_2O$ concentrations decreased rapidly far from the upstream areas (Fig. 4S(b)).

Another notable feature was that the surface $N_2O$ concentration varied over time, especially in rivers. Hot moments, or rapid temporal increases in the surface $N_2O$ concentrations, were evident in rivers (Fig. 1). There was clear seasonality for the monthly mean $N_2O$ concentration in rivers, ranging from 15 to 95 nmol $L^{-1}$, with peak concentrations being observed in the summer. In contrast to rivers, the temporal variation showed a narrower range for ponds (7–34 nmol $L^{-1}$) and the reservoir (9–30 nmol $L^{-1}$) but with peak concentrations being observed mostly in the winter. For rivers, the summertime $N_2O$ concentrations with a mean value of 48 nmol $L^{-1}$ were significantly ($p < 0.05$) higher than those in spring (19 nmol $L^{-1}$), autumn (24 nmol $L^{-1}$), and winter (28 nmol $L^{-1}$). For ponds, the summertime $N_2O$ concentration with a mean value of 16 nmol $L^{-1}$ was significant ($p < 0.05$) lower than that in winter (25 nmol $L^{-1}$). Additionally, the seasonal average values in the reservoir were 13 (spring), 18 (summer), 14 (autumn), and 18 nmol $L^{-1}$ (winter), respectively, showing significant ($p = 0.046$) difference between spring and summer. We cannot characterize the seasonal variation of $N_2O$ concentrations in ditches due to non-continuous measurements in time.

### 3.3. Relationships between $N_2O$ concentration and environment factors

Surface $N_2O$ concentration in the rivers, ponds, and reservoir exhibited different responses to inorganic N loadings (Fig. S5). The $N_2O$ concentration and $NO_3^-$-N concentration exhibited a stronger correlation in rivers ($r = 0.71$, $p < 0.01$) than in ponds ($r = 0.38$, $p = 0.03$). Inversely, a stronger correlation between $N_2O$ concentration and $NH_4^+$-N concentration was found in ponds ($r = 0.65$, $p < 0.01$) than in rivers ($r = 0.33$, $p < 0.01$). Additionally, the $NO_2^-$-N concentration was well correlated with the riverine $N_2O$ concentration ($r = 0.65$, $p < 0.01$). In the reservoir, the $N_2O$ concentrations showed no significant correlation with any form of inorganic N loadings.

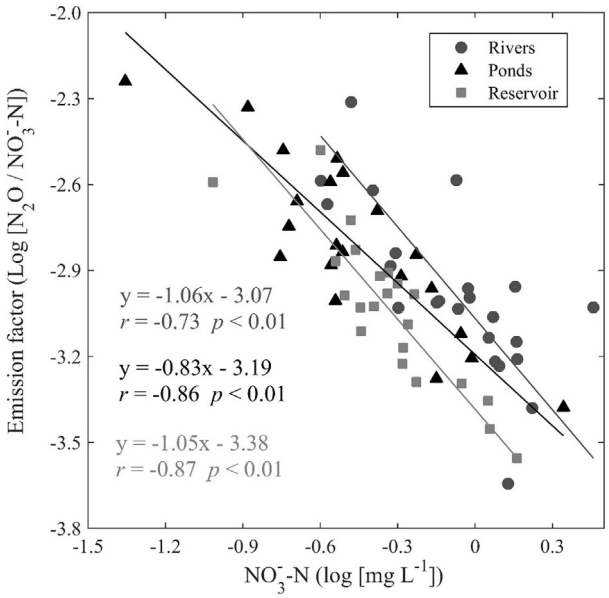


**Fig. 4.** Simple liner regression of normalized monthly mean $N_2O$ emission factor ($N_2O$-N/$NO_3^-$-N ratio) and normalized $NO_3^-$-N concentration in the collected rivers, ponds, and reservoir samples.

The temporal correlation between the surface water $N_2O$ concentration and water temperature were insignificant for rivers ($r = 0.27$, $p = 0.20$), ponds ($r = 0.37$, $p = 0.08$), and reservoir ($r = 0.11$, $p = 0.61$). Correlation analyses also revealed that the temporal variation in $N_2O$ concentration was not correlated well with the water chemical properties (e.g., Spc, pH, and DO). Precipitation, by contrast, appeared to contribute to the temporal variation of the $N_2O$ concentration (Fig. 2). The accumulated precipitation for ten days before sampling was well correlated with the monthly riverine $N_2O$ concentration when the precipitation amounts were greater than 50 mm ($r = 0.92$, $p < 0.01$). Importantly, the hot moments, the rapid temporal increase in the riverine $N_2O$ production (Fu et al., 2018), were induced by heavy precipitation during the crop-planting period in the study (Fig. 1). However, the temporal correlation between precipitation and the $N_2O$ concentration in the lentic ecosystems (ponds and reservoir) was insignificant ($p > 0.05$).

### 3.4. Indirect $N_2O$ fluxes

The mean estimated indirect $N_2O$ emission (mean ± 1 standard deviation) from the surface water of the agricultural watershed was 27.1 ± 23.4 μmol $m^{-2}$ $d^{-1}$ based on two years' field measurements. The rivers were found to have the highest $N_2O$ fluxes, with a mean value of 49.6 μmol $m^{-2}$ $d^{-1}$. Ditches had the second highest $N_2O$ fluxes with large uncertainly (mean ± 1 standard deviation: 45.2 ± 95.1 μmol $m^{-2}$ $d^{-1}$; Table 1). The ponds and reservoir showed moderate emission fluxes with a mean value of 8.0 and 5.6 μmol $m^{-2}$ $d^{-1}$, respectively. The highest $N_2O$ fluxes for the three water body types — rivers, ponds, and reservoir — were found in the summer (Table 1).

The indirect $N_2O$ fluxes from water bodies in the watershed were calculated with the dissolved $N_2O$ concentration. The calculated indirect $N_2O$ fluxes and dissolved $N_2O$ concentration were highly correlated for all records across water body types and over time ($r = 0.97$, $p < 0.01$). The roles of environment factors influencing the $N_2O$ fluxes were similar to those of surface water-dissolved $N_2O$ concentration.

### 3.5. Indirect $N_2O$ emission factor

The results revealed that the EF was not uniform for the different water types (Fig. 3). Ponds had the highest EF, followed by ditches and rivers on average (Table 1). The reservoir, the large water body in the watershed, had the lowest EF with a mean value of 0.0011. The EF of 0.0013 for rivers was nearly half of the default 0.0025 by IPCC. Additionally, the measured EF of 0.0014 for ditches was also significantly lower than the IPCC default value of 0.0025 for river.

It was evidenced from the field measurements that EF varied over time (Fig. 3). The monthly mean EF varied from 0.0002 to 0.0049 for rivers, 0.0004 to 0.0057 for ponds, and 0.0002 to 0.0033 for the reservoir over the two-year period. The riverine EF showed apparent seasonality: summer (mean ± 1 standard deviation: 0.0021 ± 0.0016) > spring (0.0015 ± 0.0007) > autumn (0.0009 ± 0.0005) > winter (0.0007 ± 0.0002, Table 1). In contrast to $N_2O$ concentration, the EFs were highly negative with the $NO_3^-$-N concentration for rivers, ponds, and the reservoir (Fig. 4).

## 4. Discussion

### 4.1. Controls on $N_2O$ variability

Previous field measurements demonstrated that although other environmental factors such as dissolved oxygen (Kampschreur et al., 2009; Rosamond et al., 2012), organic carbon (Kampschreur

et al., 2009), and water temperature (Venkiteswaran et al., 2014) affect the riverine $N_2O$ production rate, the $NO_3^-$-N concentration was the predominant control on the riverine $N_2O$ concentration in this study (Fig. S5(a)). The pattern was consistent with previous observations, showing that $NO_3^-$-N is an important driver of riverine $N_2O$ production in agricultural watersheds (Beaulieu et al., 2008; Baulch et al., 2011; Turner et al. 2016; Hama-Aziz et al., 2017; Tian et al., 2017). It is likely that farmland N fertilizer loading to rivers stimulates denitrification and associated $N_2O$ production (Kampschreur et al., 2009; Beaulieu et al. 2011; Maavara et al., 2019). $NH_4^+$-N concentrations, a good indicator of domestic pollution (Garnier et al. 2009), were found to peak in ponds (Table 1). Additionally, the strong relationship between $NH_4^+$-N and pond $N_2O$ concentration ($r = 0.65$, $p < 0.01$; Fig. S5(b)) is reasonable because the high $NH_4^+$-N level may increase the $N_2O$ accumulation via nitrification, which had been demonstrated in high population density areas (Xia et al., 2013a; Yu et al. 2013; Hu et al., 2016). The poor correlation between $N_2O$ and any form of N loading in the reservoir, by contrast, indicated that other biotic and abiotic factors played a greater role than N loading in $N_2O$ production (Deemer et al. 2016).

Both field measurement and model simulation find that the riverine $N_2O$ production rate is highly sensitive to perturbations in precipitation (Chen et al. 2016; Cooper et al., 2017; Griffis et al. 2017; Fu et al., 2018). Here, precipitation (10-day accumulated precipitation prior to sampling > 50 mm) was found to drive the temporal variation of the riverine $N_2O$ concentration (Fig. 2a), consistent with previous studies in the agriculture watersheds in Southwestern China (Tian et al., 2017) and UK (Cooper et al., 2017). Heavy precipitation is likely to transport more agricultural N loading to the river (Sinha et al., 2017, Fig. 2b) and subsequently stimulates $N_2O$ production (Liu and Greaver, 2009; Tian et al., 2017). The results reported here showed that heavy precipitation combined with intense agricultural fertilizer application during the farming season triggered riverine $N_2O$ hot moments (Fig. 1), which should be captured to reduce the uncertainty of the $N_2O$ budget (Fu et al., 2018; Shrestha and Wang, 2018). The projected increase in both heavy and total precipitation induced by climate change (Sinha et al., 2017), together with the increase in the use of nitrogen fertilizer to meet the food demand (Jiang et al., 2010; Saikawa et al. 2014), posed significant potential for agricultural watershed indirect $N_2O$ production in the global $N_2O$ budget.

Although many previous studies showed a strong positive correlation between temperature and riverine $N_2O$ production (Beaulieu et al., 2010; Hinshaw and Dahlgren, 2012; Shrestha and Wang, 2018), our results reported here were consistent with the field measurement in a Swedish agricultural catchment showing water temperature had an insignificant effect on seasonal variation of $N_2O$ concentration (Audet et al., 2017). This is probably due to the N concentration outweighs the temperature in determining the water $N_2O$ production via nitrification and denitrification (Kampschreur et al., 2009; Davidson et al. 2015; Capodici et al., 2018). Another notable feature was that the surface $NO_3^-$-N concentration in rivers was the highest in winter, but the highest $N_2O$ concentration occurred in summer in this study (Table 1). Some studies have proposed that the carbon limitation during denitrification is associated with increased $N_2O$ production (Kampschreur et al., 2009; Capodici et al., 2018), which may be the explanation for this pattern. Because study has shown that the dissolved organic carbon in these rivers increased from 6.2 mg $L^{-1}$ in summer to 18.6 mg $L^{-1}$ in winter, with the C:N ratio increased from 1.3 to 3.1 (Zhao et al., 2013). The high C:N ratio may supply availability carbon sources, resulting in an increase in denitrification efficiency and associated decrease in $N_2O$ production although the high $NO_3^-$-N concentration in winter in this study (Kampschreur et al., 2009; Zhao et al., 2013; Capodici et al., 2018).

The riverine $N_2O$ production rate varies greatly by geographic location (Fig. S4). The most notable feature was that the $N_2O$ concentration decreased sharply from the upstream to the estuary, with the mean value decreasing from 47 to 17 nmol $L^{-1}$ in River 2. The result reported here is consistent with the field measurement in other intensive agricultural activity areas, such as the Seine basin in France (Garnier et al. 2009), the U.S. Corn Belt (Turner et al., 2015), and a typical agriculture watershed in the UK (Reay et al., 2003). The high $NO_3^-$-N concentrations in upstream waters (Fig. 4S(a)), may enhance the microbial processes of $N_2O$ production (Herrman et al., 2008; Zhao et al., 2014). Notably, direct $N_2O$ input from other sources, such as soil and groundwater, might also lead to a high $N_2O$ concentration in upstream waters (Garnier et al. 2009; Beaulieu et al. 2011). As suggested in previous studies, the upstream waters are the hot spot for $N_2O$ production (Peterson et al. 2001; Turner et al., 2015). In summary, $N_2O$ production rates in hotspots were two times greater than in non-hotspot locations in the presented study.

### 4.2. Indirect $N_2O$ fluxes in the agricultural watershed

The combined indirect $N_2O$ fluxes from rivers, ponds, and reservoir were calculated to be 383 kg $N_2O$-N $yr^{-1}$. The rivers were the most significant contributor of $N_2O$ fluxes of all water bodies, contributing to a total of 161 kg $N_2O$-N $yr^{-1}$. Total direct $N_2O$ fluxes from the watershed fertilized soil was estimated to be 12 t ($10^3$ kg) N $yr^{-1}$ in the watershed (Xia et al., 2013b). Based on a study in another similar region in Eastern China (She et al. 2018), we roughly estimated that the ditch area for the rice-wheat field is 25 $hm^2$. Adding the annul $N_2O$ emission yield from agriculture ditches (~117 kg $N_2O$-N $yr^{-1}$) in the watershed, the watershed indirect $N_2O$ emission thus represents approximately 4% of the total $N_2O$ emissions from N-fertilizer. Although the obtained percentage was similar to other studies (Beaulieu et al., 2008; Garnier et al. 2009; Audet et al., 2017), caution should be taken for the following reasons: (1) the ditch areas and $N_2O$ emission rates ($45.2 \pm 95.1$ μmol $m^{-2}$ $d^{-1}$) had large uncertainly; (2) the presented sampling strategies might omit some riverine emission hot spots and hot moments, which may lead to low biases in the annual total $N_2O$ emission yield (Fu et al., 2018).

For lentic ecosystems, the annual mean $N_2O$ emission rates in ponds and reservoir (8.0 and 5.6 μmol $m^{-2}$ $d^{-1}$, respectively) were higher than the median emission rate (3.9 μmol $m^{-2}$ $d^{-1}$) in global lakes/reservoirs according to Hu et al. (2016). Meanwhile, these values were also higher than those in temperature lakes with a mean value of 3.4 μmol $m^{-2}$ $d^{-1}$ (Soued et al., 2016). A heavily polluted lake nearby, Lake Taihu, showed a moderate $N_2O$ emission of 3.5 μmol $m^{-2}$ $d^{-1}$ (Xiao et al., 2019). The gas transfer velocity of a lentic ecosystem in the study region can be accurately estimated using the wind-dependent formula, which had been demonstrated previously (Xiao et al. 2017). These results together indicated watershed N inputs fueled the pond and reservoir $N_2O$ emission.

The indirect riverine $N_2O$ fluxes reported here is compared to the results reported by previous studies (Table S1). The literature review in Table S1 showed that the riverine $N_2O$ fluxes across multiple land-use types ranged from 6.7 to 121.3 μmol $m^{-2}$ $d^{-1}$, with a mean value of 51.3 μmol $m^{-2}$ $d^{-1}$. Based on a meta-analysis with 169 observations, the global median riverine $N_2O$ emission fluxes is 14.4 μmol $m^{-2}$ $d^{-1}$, which is significantly lower than the annual mean flux reported here (49.6 μmol $m^{-2}$ $d^{-1}$). For comparison, the direct $N_2O$ emission rate from fertilized soil in the study area is approximately 60–90 μmol $m^{-2}$ $d^{-1}$ (Zou et al., 2005; Zhou et al. 2014; Liu et al., 2016). Therefore, indirect $N_2O$ emissions caused by N leaching and surface runoff N losses in agriculture

watershed could contribute significantly to the total $N_2O$ emission.

The $N_2O$ emissions from water are often determined by water-air gas exchange model or direct field measurement such as using floating chamber technique (Outram and Hiscock, 2012; Zhu et al. 2015; Hama-Aziz et al., 2017; Wu et al., 2018; Capodici et al., 2018). The water-air gas exchange model has been frequently employed to quality $N_2O$ emission flux from water, accounting for 80% of flux measurements (Hu et al., 2016; Wu et al., 2018), however, the model-based method may either overestimate or underestimate $N_2O$ emission due to the uncertainly in gas transfer coefficient (Yu et al. 2013; Raymond et al. 2013; Wu et al., 2018). For comparison, the direct measurement using floating chamber method showed the $N_2O$ emission flux were 48.1–66.1 μmol $m^{-2}$ $d^{-1}$ and below 8.6 μmol $m^{-2}$ $d^{-1}$ from the rivers and ponds, respectively, within the same watershed (Li et al., 2011; Xia et al., 2013a; Han et al., 2014), which were similar to the model-estimated $N_2O$ emission flux in the presented study (river: 49.6 μmol $m^{-2}$ $d^{-1}$; ponds: 8.0 μmol $m^{-2}$ $d^{-1}$). Additionally, previous study has shown that the $N_2O$ emission flux measured by the two methods above exhibits the same seasonal variation in an agricultural watershed in southeast China (Wu et al., 2018). Both of these indicate the model-based method was reasonable for quantifying the watershed indirect $N_2O$ emission in this study.

### 4.3. Implication of the measured EF values

This study revealed that indirect $N_2O$ EFs were not uniform for the different surface water types within the same watershed (Table 1 and Fig. 3). This is consistent with the field measurement in UK agriculture watershed, which shows that different water types produce various amounts of $N_2O$ (Outram and Hiscock, 2012; Hama-Aziz et al., 2017). Therefore, separate EFs for each water compartment are required to better understand the indirect $N_2O$ budget. Emission factor for lentic ponds and the reservoir should also be included because our results showed that ignoring the indirect $N_2O$ emission from the lentic ecosystems would lead to an underestimation of the indirect emission yield by 60%.

For rivers and ditches, the EF values of 0.0013 and 0.0014 were both lower than the IPCC EF value of 0.0025. These results indicated that the IPCC default value of 0.0025 may overestimate the agriculture watershed indirect $N_2O$ emission in the study region. The recent study by Maavara et al., (2019) using mechanistic modeling approach also showed IPCC EFs are likely overestimated. Meanwhile, our data showed that the EF value across different water types varied over time with a peak appearing in the summer (Fig. 3), which is consistent with a previous study (Hama-Aziz et al., 2017). Thus, it may be more applicable to have more measurements across different seasons. Meanwhile, we also found that the IPCC approach of using one EF for all rivers may be inappropriate because EFs were highly variable across rivers, as suggested by Beaulieu et al. (2008). The EF values for rivers 1 2, and 3 were 0.0015, 0.0011, and 0.0016, respectively. Since there are no IPCC EFs for the ponds and reservoir (Outram and Hiscock, 2012), a comparison cannot be made. However, a synthesis analysis showed that EF for ponds and reservoirs was 0.0012 (Tian et al., 2018), which was significantly lower than that reported EF value of pond (0.0020) but was same as the value of reservoir in this study.

Compared to the previous results, many studies have also observed lower EFs than the IPCC default value; however, other studies showed higher EFs (Table S1). These inconsistent reports may be reasonable, because a meta-analysis of global data found that riverine $N_2O$ EFs varied across regions (Hu et al., 2016). Meanwhile, our data showed significant negative relationships between EF and N loading (Fig. 4), which is consistent with some previous studies (Beaulieu et al. 2011; Hinshaw and Dahlgren, 2012; Hu et al., 2016). This can be attributed to decreasing microbial activity with increasing N input due to progressive biological saturation (Hu et al., 2016; Mulholland et al. 2008). Although previous studies found that large rivers had low EF (Fu et al., 2018; Hinshaw and Dahlgren, 2012), we proposed that the lower EF may appear in watersheds with a high anthropogenic N input (Fig. 4), highlighting potential constraints in the IPCC methodology for rivers with high N loading. For example, in China, the annual mean riverine $N_2O$ EF in this agriculture watershed with a high N fertilizer rate (~600 kg N $ha^{-1}$ $yr^{-1}$) was 0.0013, but in the center of the Sichuan Basin with a relatively low N fertilizer rate (~280 kg N $ha^{-1}$ $yr^{-1}$) (Zhou et al. 2012), the value was 0.0027 (Tian et al., 2017).

## 5. Conclusions

Two years' field measurements in the watershed, an intensively agricultural region located in Eastern China, showed the surface $N_2O$ concentrations and fluxes varied seasonally and spatially. The annual mean surface dissolved $N_2O$ concentrations for rivers, ponds, reservoir, and ditches were 30 nmol $L^{-1}$, 19 nmol $L^{-1}$, 16 nmol $L^{-1}$, and 58 nmol $L^{-1}$, corresponding to the computed $N_2O$ fluxes of 49.6 μmol $m^{-2}$ $d^{-1}$, 8.0 μmol $m^{-2}$ $d^{-1}$, 5.6 μmol $m^{-2}$ $d^{-1}$, and 45.2 μmol $m^{-2}$ $d^{-1}$, respectively.

Dissolved $N_2O$ concentration can be best predicted by $NO_3^-$-N concentrations in rivers ($r = 0.71$, $p < 0.02$) and by $NH_4^+$ in ponds ($r = 0.65$, $p < 0.01$). The temporal variation of the riverine $N_2O$ concentration appears to be controlled by precipitation, and heavy precipitation induced the emission hot moments during the farming season. Upstream waters are the hot spots in which riverine $N_2O$ production rates were two times greater than in non-hotspot locations.

The modeled watershed indirect $N_2O$ emission fluxes were comparable to the direct emission fluxes from the fertilized soils. A coarse estimate suggests that indirect $N_2O$ emissions represent approximately 4% of the total $N_2O$ emissions from N-fertilizer at the watershed scale. However, the IPCC default value of 0.0025 may overestimate the agriculture watershed indirect $N_2O$ emission in the study region. We propose that separate EFs for different seasons and different water types may be more appropriate due to the large variability.

## Acknowledgements

This study was supported jointly by the National Natural Science Foundation of China (41775152, 41775151, 41801093) and the China Postdoctoral Science Foundation (2018M632404). We thank the staff of the Yale-NUIST Center on Atmospheric Environment for their assistance with field sample collection and laboratory measurements.

## Appendix A. Supplementary data

Supplementary data to this article can be found online at https://doi.org/10.1016/j.envpol.2019.04.076.

## References

Audet, J., Wallin, M.B., Kyllmar, K., Andersson, S., Bishop, K., 2017. Nitrous oxide emissions from streams in a Swedish agricultural catchment. Agric. Ecosyst. Environ. 236, 295–303.

Baulch, H.M., Schiff, S.L., Maranger, R., Dillon, P.J., 2011. Nitrogen enrichment and the emission of nitrous oxide from streams. Glob. Biogeochem. Cycles 25.

Beaulieu, J.J., Arango, C.P., Hamilton, S.K., Tank, J.L., 2008. The production and emission of nitrous oxide from headwater streams in the Midwestern United States. Glob. Chang. Biol. 14, 878–894.

Beaulieu, J.J., Shuster, W.D., Rebholz, J.A., 2010. Nitrous oxide emissions from a large, impounded river: the Ohio river. Environ. Sci. Technol. 44, 7527–7533.

Beaulieu, J.J., et al., 2011. Nitrous oxide emission from denitrification in stream and river networks. Proc. Natl. Acad. Sci. U.S.A. 108, 214–219.
Borges, A.V., et al., 2015. Globally significant greenhouse-gas emissions from African inland waters. Nat. Geosci. 8, 637–642.
Capodici, M., Avona, A., Laudicina, V.A., Viviani, G., 2018. Biological groundwater denitrification systems: lab-scale trials aimed at nitrous oxide production and emission assessment. Sci. Total Environ. 630, 462–468.
Chen, Z., et al., 2016. Partitioning $N_2O$ emissions within the US Corn Belt using an inverse modeling approach. Glob. Biogeochem. Cycles 30, 1192–1205.
Clough, T.J., Buckthought, L.E., Kelliher, F.M., Sherlock, R.R., 2007. Diurnal fluctuations of dissolved nitrous oxide ($N_2O$) concentrations and estimates of $N_2O$ emissions from a spring-fed river: implications for IPCC methodology. Glob. Chang. Biol. 13, 1016–1027.
Cole, J.J., Caraco, N.F., 1998. Atmospheric exchange of carbon dioxide in a low-wind oligotrophic lake measured by the addition of $SF_6$. Limnol. Oceanogr. 43, 647–656.
Cooper, R.J., Wexler, S.K., Adams, C.A., Hiscock, K.M., 2017. Hydrogeological controls on regional-scale indirect nitrous oxide emission factors for rivers. Environ. Sci. Technol. 51, 10440–10448.
Davidson, E.A., 2009. The contribution of manure and fertilizer nitrogen to atmospheric nitrous oxide since 1860. Nat. Geosci. 2, 659–662.
Davidson, T.A., et al., 2015. Eutrophication effects on greenhouse gas fluxes from shallow-lake mesocosms override those of climate warming. Glob. Chang. Biol. 21, 4449–4463.
De Klein, C., et al., 2006. $N_2O$ emissions from managed soils, and $CO_2$ emissions from lime and urea application. IPCC Guidelines for National Greenhouse Gas Inventories, Prepared by the National Greenhouse Gas Inventories Programme, 4, pp. 1–54.
Deemer, B.R., et al., 2016. Greenhouse gas emissions from reservoir water surfaces: a new global synthesis. BioScience 66, 949–964.
Fu, C., Lee, X., Griffis, T.J., Baker, J.M., Turner, P.A., 2018. A modeling study of direct and indirect $N_2O$ emissions from a representative catchment in the U.S. Corn Belt. Water Resour. Res. 54.
Fu, C., Lee, X., Griffis, T.J., Dlugokencky, E.J., Andrews, A.E., 2017. Investigation of the $N_2O$ emission strength in the U. S. Corn Belt. Atmos. Res. 194, 66–77.
Garnier, J., et al., 2009. Nitrous oxide ($N_2O$) in the Seine river and basin: observations and budgets. Agric. Ecosyst. Environ. 133, 223–233.
Griffis, T.J., et al., 2017. Nitrous oxide emissions are enhanced in a warmer and wetter world. Proc. Natl. Acad. Sci. U.S.A. 114, 12081–12085.
Hama-Aziz, Z.Q., Hiscock, K.M., Cooper, R.J., 2017. Indirect nitrous oxide emission factors for agricultural field drains and headwater streams. Environ. Sci. Technol. 51, 301–307.
Han, Y., Zheng, Y., Wu, R., Yin, J., Sun, X., 2014. Nitrous oxide flux at the water-air interface of the river in Nanjing during summer. Environ. Sci. 35, 348–355 (In Chinese).
Herrman, K.S., Bouchard, V., Moore, R.H., 2008. Factors affecting denitrification in agricultural headwater streams in Northeast Ohio, USA. Hydrobiologia 598, 305–314.
Hinshaw, S.E., Dahlgren, R.A., 2012. Dissolved nitrous oxide concentrations and fluxes from the eutrophic San Joaquin River, California. Environ. Sci. Technol. 47, 1313–1322.
Hu, M., Chen, D., Dahlgren, R.A., 2016. Modeling nitrous oxide emission from rivers: a global assessment. Glob. Chang. Biol. 22, 3566–3582.
Jiang, J., Hu, Z., Sun, W., Huang, Y., 2010. Nitrous oxide emissions from Chinese cropland fertilized with a range of slow-release nitrogen compounds. Agric. Ecosyst. Environ. 135, 216–225.
Ju, X.T., et al., 2009. Reducing environmental risk by improving N management in intensive Chinese agricultural systems. Proc. Natl. Acad. Sci. U.S.A. 106, 3041–3046.
Kampschreur, M., Temmink, H., Kleerebezem, R., Jetten, M., Loosdrecht, M., 2009. Nitrous oxide emission during wastewater treatment. Water Res. 43, 4093–4103.
Kroeze, C., Mosier, A., Bouwman, L., 1999. Closing the global $N_2O$ budget: a retrospective analysis 1500-1994. Glob. Biogeochem. Cycles 13, 1–8.
Li, F., Wang, J., Li, X., Xiao, X., Zou, H., Li, F., 2011. $N_2O$ emission from pond and river in the agricultural watershed of Jurong reservoir, Jiangsu Province. Acta Sci. Circumstantiae 31, 2022–2027 (In Chinese).
Liu, L., Greaver, T.L., 2009. A review of nitrogen enrichment effects on three biogenic GHGs: the CO2 sink may be largely offset by stimulated $N_2O$ and $CH_4$ emission. Ecol. Lett. 12, 1103–1117.
Liu, S., Hu, Z., Wu, S., Li, S., Li, Z., Zou, J., 2016. Methane and nitrous oxide emissions reduced following conversion of rice paddies to inland crab fish aquaculture in southeast China. Environ. Sci. Technol. 50, 633–642.
Maavara, T., Lauerwald, R., Laruelle, G., Akbarzadeh, Z., Bouskill, N., Cappellen, P., Regnier, P., 2019. Nitrous oxide emissions from inland waters: are IPCC estimates too high? Glob. Chang. Biol. 25, 473–488.
Mosier, A., Kroeze, C., Nevison, C., Oenema, O., Seitzinger, S., van Cleemput, O., 1998. Closing the global $N_2O$ budget: nitrous oxide emissions through the agricultural nitrogen cycle. Nutrient Cycl. Agroecosyst. 52, 225–248.
Mulholland, P.J., et al., 2008. Stream denitrification across biomes and its response to anthropogenic nitrate loading. Nature 452, 202–205.
Outram, F.N., Hiscock, K.M., 2012. Indirect nitrous oxide emissions from surface water bodies in a lowland arable catchment: a significant contribution to agricultural greenhouse gas budgets? Environ. Sci. Technol. 46, 8156–8163.
Peterson, B.J., et al., 2001. Control of nitrogen export from watersheds by headwater streams. Science 292, 86–90.
Ravishankara, A.R., Daniel, J.S., Portmann, R.W., 2009. Nitrous oxide ($N_2O$): the dominant ozone-depleting substance emitted in the 21st century. Science 326, 123–125.
Raymond, P.A., et al., 2013. Global carbon dioxide emissions from inland waters. Nature 503, 355–359.
Reay, D.S., et al., 2012. Global agriculture and nitrous oxide emissions. Nat. Clim. Change 2, 410–416.
Reay, D.S., Smith, K.A., Edwards, A.C., 2003. Nitrous oxide emission from agricultural drainage waters. Glob. Chang. Biol. 9, 195–203.
Rosamond, M.S., Thuss, S.J., Schiff, S.L., 2012. Dependence of riverine nitrous oxide emissions on dissolved oxygen levels. Nat. Geosci. 5, 715–718.
Saikawa, E., et al., 2014. Global and regional emissions estimates for $N_2O$. Atmos. Chem. Phys. 14, 4617–4641.
Seitzinger, S.P., Kroeze, C., 1998. Global distribution of nitrous oxide production and N inputs in freshwater and coastal marine ecosystems. Glob. Biogeochem. Cycles 12, 93–113.
Shcherbak, I., Millar, N., Robertson, G.P., 2014. Global metaanalysis of the nonlinear response of soil nitrous oxide ($N_2O$) emissions to fertilizer nitrogen. Proc. Natl. Acad. Sci. U.S.A. 111, 9199–9204.
She, D., et al., 2018. Limited N removal by denitrification in agricultural drainage ditches in the Taihu Lake region of China. J. Soils Sediments 18, 1110–1119.
Shrestha, N.K., Wang, J., 2018. Current and future hot-spots and hot-moments of nitrous oxide emission in a cold climate river basin. Environ. Pollut. 239, 648–660.
Sinha, E., Michalak, A.M., Balaji, V., 2017. Eutrophication will increase during the 21st century as a result of precipitation changes. Science 357, 405–408.
Soued, C., del Giorgio, P.A., Maranger, R., 2016. Nitrous oxide sinks and emissions in boreal aquatic networks in Québec. Nat. Geosci. 9, 116–120.
Tian, L., Cai, Y., Akiyama, H., 2018. A review of indirect $N_2O$ emission factors from agricultural nitrogen leaching and runoff to update of the default IPCC values. Environ. Pollut. 245, 300–306.
Tian, L.L., Zhu, B., Akiyama, H., 2017. Seasonal variations in indirect $N_2O$ emissions from an agricultural headwater ditch. Biol. Fertil. Soils 53, 651–662.
Turner, P.A., et al., 2016. Regional-scale controls on dissolved nitrous oxide in the Upper Mississippi River. Geophys. Res. Lett. 43, 4400–4407.
Turner, P.A., Griffis, T.J., Lee, X., Baker, J.M., Venterea, R.T., Wood, J.D., 2015. Indirect nitrous oxide emissions from streams within the US Corn Belt scale with stream order. Proc. Natl. Acad. Sci. U.S.A. 112, 9839–9843.
Venkiteswaran, J.J., Rosamond, M.S., Schiff, S.L., 2014. Nonlinear response of riverine N2O fluxes to oxygen and temperature. Environ. Sci. Technol. 48, 1566–1573.
Wu, S., Chen, J., Li, C., Kong, D., Yu, K., Liu, S., Zou, J., 2018. Diel and seasonal nitrous oxide fluxes determined by floating chamber and gas transfer equation methods in agricultural irrigation watersheds in southeast China. Environ. Monit. Assess. 190, 122.
Xia, Y., Li, Y., Li, X., Guo, M., She, D., Yan, X., 2013a. Diurnal pattern in nitrous oxide emissions from a sewage-enriched river. Chemosphere 92, 421–428.
Xia, Y.Q., Li, Y.F., Ti, C.P., Li, X.B., Zhao, Y.Q., Yan, X.Y., 2013b. Is indirect $N_2O$ emission a significant contributor to the agricultural greenhouse gas budget? A case study of a rice paddy-dominated agricultural watershed in eastern China. Atmos. Environ. 77, 943–950.
Xiao, Q., et al., 2017. Spatial variations of methane emission in a large shallow eutrophic lake in subtropical climate. J. Geophys. Res.-Biogeo. 122, 1597–1614.
Xiao, Q., Xu, X., Zhang, M., Duan, H., Hu, Z., Wang, W., Xiao, W., Lee, X., 2019. Coregulation of nitrous oxide emissions by nitrogen and temperature in China's third largest freshwater lake (Lake Taihu). Limnol. Oceanogr. https://doi.org/10.1002/lno.11098.
Xing, G.X., Zhu, Z.L., 2002. Regional nitrogen budgets for China and its major watersheds. Biogeochemistry 57, 405–427.
Xu, X., Tian, H., Hui, D., 2008. Convergence in the relationship of $CO_2$ and $N_2O$ exchanges between soil and atmosphere within terrestrial ecosystems. Glob. Chang. Biol. 14, 1651–1660.
Yan, X., et al., 2011. Nitrogen budget and riverine nitrogen output in a rice paddy dominated agricultural watershed in eastern China. Biogeochemistry 106, 489–501.
Yu, Z., et al., 2013. Nitrous oxide emissions in the Shanghai river network: implications for the effects of urban sewage and IPCC methodology. Glob. Chang. Biol. 19, 2999–3010.
Zhao, Y., Xia, Y., Li, B., Yan, X., 2014. Influence of environmental factors on net $N_2$ and $N_2O$ production in sediment of freshwater rivers. Environ. Sci. Pollut. Res. 21, 9973–9982.
Zhao, Y., Xia, Y., Kana, T., Wu, Y., Li, X., Yan, X., 2013. Seasonal variation and controlling factors of anaerobic ammonium oxidation in freshwater river sediments in the Taihu Lake region of China. Chemosphere 93, 2124–2131.
Zhou, F., et al., 2014. A new high-resolution $N_2O$ emission inventory for China in 2008. Environ. Sci. Technol. 48, 8538–8547.
Zhou, M., et al., 2012. Nitrate leaching, direct and indirect nitrous oxide fluxes from sloping cropland in the purple soil area, southwestern China. Environ. Pollut. 162, 361–368.
Zhu, D., et al., 2015. Nitrous oxide emission from infralittoral zone and pelagic zone in a shallow lake: implications for whole lake flux estimation and lake restoration. Ecol. Eng. 82, 368–375.
Zou, J.W., Huang, Y., Jiang, J.Y., Zheng, X.H., Sass, R.L., 2005. A 3-year field measurement of methane and nitrous oxide emissions from rice paddies in China: effects of water regime, crop residue, and fertilizer application. Glob. Biogeochem. Cycles 19.